REPORT DOCUMENTATION PAGE

Form Approved
OMB No. 0704-0188

1. AGENCY USE ONLY (Leave blank)	2. REPORT DATE	3. REPORT TYPE AND DATES COVERED
	January 1996	Technical

4. TITLE AND SUBTITLE
Quantitative Interpretation of K-Edge NEXAFS Data for Various Nickel Hydroxides and the Charged Nickel Electrode

5. FUNDING NUMBERS
Grant #:
N00014-93-1-0331

6. AUTHOR(S)
X. Qian, H. Sambe and D.E. Ramaker

7. PERFORMING ORGANIZATION NAME(S) AND ADDRESS(ES)
Department of Chemistry
The George Washington University
Washington, D.C. 20052

8. PERFORMING ORGANIZATION REPORT NUMBER
Technical Report
#73

9. SPONSORING/MONITORING AGENCY NAME(S) AND ADDRESS(ES)
Office of Naval Research
800 N. Quincy Street
Arlington, VA 22217-5000

10. SPONSORING/MONITORING AGENCY REPORT NUMBER
R&T Code: 4133044

11. SUPPLEMENTARY NOTES

12a. DISTRIBUTION/AVAILABILITY STATEMENT
Approved for public release; distribution is unlimited.

12b. DISTRIBUTION CODE
Unlimited

13. ABSTRACT *(Maximum 200 words)*

A quantitative interpretation of Ni K-edge NEXAFS data for β-$Ni(OH)_2$, β-NiOOH, and $BaNiO_3$, and *in situ* data for a charged Ni electrode is reported. We have performed curve-wave multiple scattering calculations utilizing the FEFF6 code on clusters approximating these materials. These theoretical results reproduce the experimental changes with oxidation remarkably well. Our interpretation of the NEXAFS line shape for the charged electrode indicates that large amounts of Ni^{+4} exists along with $Ni^{+3.3}$, giving an average oxidation slightly greater than 3.5, consistent with that shown elsewhere from the edge shift data.

14. SUBJECT TERMS	15. NUMBER OF PAGES
Nickel Hydroxides, nickel electrode, NEXAFS	16. PRICE CODE

17. SECURITY CLASSIFICATION OF REPORT	18. SECURITY CLASSIFICATION OF THIS PAGE	19. SECURITY CLASSIFICATION OF ABSTRACT	20. LIMITATION OF ABSTRACT
unclassified	unclassified	unclassified	unclassified

OFFICE OF NAVAL RESEARCH

GRANT: N00014-93-1-0331

R&T Code 4133044

TECHNICAL REPORT No. 73

Quantitative Interpretation of K-Edge NEXAFS Data for Various Nickel Hydroxides and the Charged Nickel Electrode

by

X. Qian, H. Sambe, and D.E. Ramaker

Prepared for Publication in
Journal of Physical Chemistry

Department of Chemistry
George Washington University
Washington, DC 20052

January 1996

QUANTITATIVE INTERPRETATION OF K-EDGE NEXAFS DATA FOR VARIOUS NICKEL HYDROXIDES AND THE CHARGED NICKEL ELECTRODE*

X. Qian, H. Sambe, and D.E. Ramaker,

Chemistry Department
George Washington University
Washington, DC 20052

and

K.I. Pandya and W.E. O'Grady

Surface Chemistry Branch, Code 6170
Naval Research Laboratory
Washington, DC 20375

ABSTRACT

A quantitative interpretation of Ni K-edge NEXAFS data for β-$Ni(OH)_2$, β-NiOOH, and $BaNiO_3$, and *in situ* data for a charged Ni electrode is reported. We have performed curve-wave multiple scattering calculations utilizing the FEFF6 code on clusters approximating these materials. These theoretical results reproduce the experimental changes with oxidation remarkably well. Our interpretation of the NEXAFS line shape for the charged electrode indicates that large amounts of Ni^{+4} exists along with $Ni^{+3.3}$, giving an average oxidation slightly greater than 3.5, consistent with that shown elsewhere from the edge shift data.

*Support from the Office of Naval Research is gratefully acknowledged.

1. INTRODUCTION

Nickel hydroxides are important materials with applications in nickel batteries,[1] fuel cell electrodes,[2] electrolyzers[3] and electrochromic devices.[4] As a result, many studies have been reported on these materials, including infra-red (IR),[5] Raman,[6,7] X-ray diffraction (XRD),[8] and near edge[9,10]and extended[11 12,13], x-ray absorption spectroscopy (NEXAFS and EXAFS), as well as several electrochemical studies.[14,15] Despite these many studies, extending over nearly a century, there are still many unanswered questions and controversies concerning these materials. Some of the problems arise because many structural phases exist (e.g. α- and β-$Ni(OH)_2$, and α-, β-, and γ-NiOOH) and the dominant phase depends on the method of preparation. Furthermore, the crystallinity of these phases are often inherently poor, and for the charged Ni electrode the data must be collected in-situ. Reviews have been published summarizing the extensive literature, the problems, and the questions that remain[15].

In this work, we will concentrate on the Ni electrode, and in particular the oxidation of β-$Ni(OH)_2$ to β-NiOOH or beyond that to a higher oxidation state. The nanostructure of the nickel electrode can be simply described as a layered structure of slabs consisting of three atomic sheets, O-Ni-O. Interspersed between the slabs are "galleries" in which various mobile species may reside[16]. The Ni atoms, lying between the hexagonally close-packed sheets of O, occupy essentially all of the octahedral positions. In the reduced form, β-$Ni(OH)_2$, the gallery is filled with H atoms; i.e., each O atom is

bonded to one H atom. Thus β-$Ni(OH)_2$ is generally well ordered crystallographically within the slabs (although some variation in the registry of the slabs and the widths of the galleries between the slabs can occur), a reasonably good XRD pattern is obtained, and its structure is well-characterized[8,9,11-13,15].

The oxidation of the Ni electrode involves the removal of H^+ ions from the gallery and transfer into the electrolyte. The extent of this H removal (1/2 to 3/4 of the total), and the positions occupied by the remaining H atoms are still open to question. Indication exists from XRD and EXAFS data that the remaining H atom distribution is rather disordered; hence the lack of crystallinity even within the O-Ni-O slabs of β-NiOOH or in the fully charged electrode[8,9,11-13,15]. This lack of crystallinity has prevented complete structural characterization with XRD data; and in particular prevents knowledge of the location and distribution of the H atoms. Finally $BaNiO_3$ has a rather different structure, with columns of NiO_6 octahedra lined face-to-face, instead of edge-to-edge as in the slabs of $Ni(OH)_2$, giving a well-ordered material and a sharp XRD pattern[9,17].

The extent of H removal and its distribution in the Ni hydroxides raises many questions in addition to those above. In particular, what factors prevent further H removal from the charged electrode, giving a higher Ni oxidation state? These questions are crucial to the functioning of a battery containing a Ni electrode, because if further H atoms could be removed, the specific capacity of the battery could be increased. For example, if instead of removing just 1/2 of the H atoms, 3/4 of them could be removed, the specific energy of the battery could be increased by 50%.

In previous work, the extent of H removal has been considered in the context of the nominal oxidation of the Ni atoms. Thus β-$Ni(OH)_2$ has nominal Ni^{+2} ions, and NiOOH has Ni^{+3} present. We will comment elsewhere on the appropriateness of this Ni oxidation picture[18]. Nevertheless within this context, if oxidation beyond Ni^{+3} could be achieved, this would suggest the existence of Ni^{+4}. Several papers have previously been published asserting evidence for the presence of Ni^{+4}[6,7,9,10,14]. Perhaps the strongest evidence for this comes from the NEXAFS edge shift[9]. In these NEXAFS edge studies, the edge is seen to shift by about 1 eV upward for each increase by one in Ni oxidation state, where the edge data for β-$Ni(OH)_2$, β-NiOOH, and $BaNiO_3$ were used for the standards of Ni in the 2,3, and 4 oxidation states respectively[9]. Using this scale, the Ni in the charged Ni electrode was seen to have an oxidation state of 3.5, consistent with previous electrochemical measurements[14].

Ni K-edge NEXAFS data has previously been published[9,10], but it was not thoroughly interpreted. In this work we use curved-wave multiple scattering calculations on the appropriate atomic clusters to interpret the NEXAFS data for β-$Ni(OH)_2$, β-NiOOH, $BaNiO_3$, and the charged electrode. We and others have shown that a detailed interpretation of NEXAFS data allows small distortions from octahedral or tetrahedral symmetry to be determined.[19,20,21] In the Ni hydroxides, these distortions are generally interpreted as arising from the differences between the Ni-O and Ni-OH bonds. Thus the Ni-O bond is elongated to 2.07 A° when a H^+ atom in the gallery is bonded to the O atom, as opposed to 1.88 A° when the O atom is not bonded to a H atom in the gallery. Although EXAFS can provide a measure of the average number of long and short Ni-O

bonds, as reported[11,12], the distribution of these long and short bonds about each Ni atom is not provided by EXAFS. We will provide some qualitative information on these distributions from a detailed interpretation of the NEXAFS data. Furthermore, we will discuss the evidence in the NEXAFS line shape for the presence of Ni^{+4} in the charged electrode.

2. EXPERIMENT AND THEORY

The experimental NEXAFS data are taken from O'Grady et al.[9] where the preparation methods for the standard materials are given in detail. XAS data were obtained for the Ni oxide battery electrodes by recording the data *in situ* immediately after charging to avoid any possible self-discharge. The experimental details concerning the cell and electrode preparation have been published earlier[12].

Curved-wave, multiple-scattering (CW-MS) cluster calculations utilizing the FEFF6 code developed by Rehr and Albers[22,23,24] were performed in this work. We have previously[19-21] performed FEFF6 calculations on alkali halides and condensed rare gases (particularly Ne) to test the validity of this code and found that the code reproduces almost all of the experimentally observed peaks except localized excitonic peaks very near the edge in some cases. Generally the absolute energy must be shifted by 0-5 eV for optimum agreement with experiment[19-24]. Furthermore, the calculated χ function generally agrees better with experiment than the absorption coefficient, $\mu = \mu_o(1+\chi)$, because of uncertainties in the atomic absorption coefficient μ_o as pointed out by Rehr et al[22-24]. We

find it convenient to compare the differences between μ, that is Δμ, for the different Ni hydroxides studied. Δμ also has μ_o removed, and it emphasizes the small differences seen with oxidation in both the experimental and theoretical NEXAFS spectra. Indeed, the difference spectra reveal features that go completely unnoticed in μ.

The input parameters for the theoretical calculations include: the atomic number of each unique atom in the cluster, the coordinates of each atom in the cluster, the choice of exchange potential (Hedin-Lundquest, Dirac-Hara, or ground state), the maximum path length, criteria for the path filter which determines the amount of multiple scattering, the Debye Waller factor (σ^2), and the charge on the ions (only positive integers allowed by the code, so we used zero in all cases). We utilized the Hedin-Lundquest potential consistent with previous experience which indicates that this potential provides the best agreement with experiment[19-24]. The maximum path length was set to 8-10 A° for the 1 and 2 shell calculations, and to 15A° for the 9 shell calculations. The path filter was chosen to be 2% for the plane waves and 1% for the curved waves (i.e. 1/2 of the default values) to include all important multiple scattering paths. The Debye Waller factor was set to 0.007[11,12].

Clusters containing 1, 2, and 9 shells of atoms were used for the calculations. The structures of β-$Ni(OH)_2$ and $BaNiO_3$ are well known from XRD data[8,17] so that up to 9 shells were used for these cases. However, β-NiOOH is not well ordered so that the long range structure is not known, indeed even the Ni coordination is not known. Recent EXAFS results[11,12] have shown an average of 3 long (2.07 A°) and 3 short (1.88 A°) Ni-O bonds about each Ni atom. Therefore FEFF6 calculations were performed on just the 1

shell clusters for this case to explore the effects of the bond length and arrangement of the bonds in the octahedral coordination about the Ni atom.

For the one-shell clusters, we utilize a notation $[nl,ns]_{cis}$ that indicates the number of long and short Ni-O bonds about the Ni atom to differentiate the calculations. It should be noted that two possible arrangements of the [3l,3s] bonds can exist about a Ni atom, namely where three long --or three short-- bonds lie in a plane (we call this the 'cis' arrangement since the long --or short-- bonds are neighboring to each other), or where two long and two short bonds are opposite each other (the 'trans' arrangement). Similarly two arrangements of the [4l,2s] or [2l,4s] exist; namely, where the two long (or 2 short) bonds are opposite (trans) or neighboring (cis) to each other. We find from the NEXAFS calculations that these cis and trans arrangements introduce relatively small differences (peaks of 5% amplitudes) compared with the 10-20 % differences noted in Figs. 2 below. Therefore, the larger effects resulting from the number of short bonds (i.e. oxidation) will be examined first, followed by an examination of the smaller effects coming from the cis or trans arrangements of these long and short bonds.

3. RESULTS AND DISCUSSION

Figure 1 shows the experimental data, μ, for the 3 standard materials and the charged electrode. Fig. 2 compares the experimental and theoretical difference spectra μ-$\mu(Ni(OH)_2)$ for the standard materials. The FEFF6 results have been optimally aligned with the experimental data for $Ni(OH)_2$. No additional energy shifts were allowed for the

NiOOH and $BaNiO_3$ data. The over all step heights in the theoretical and experimental absorption coefficients ,μ, were normalized to be one at an energy well above the edge (100 eV for the theory, 50 eV for the experimental). Thus the amplitudes in the experimental and theoretical difference curves, $\Delta\mu$, reported in Figs. 2 and 3 are absolute. The FEFF6 $\Delta\mu$ spectra above 100 eV reveal only very small oscillations about zero (i.e. EXAFS oscillations). The experimental $\Delta\mu$ spectra have had a small straight line background of optimal slope removed to assure the same behavior, consistent with the usual treatment in EXAFS calculations.

Figure 2 reveals several interesting features:

a. First the magnitude of the negative going peak around 15 eV indicates the extent of the upward shift of the edge with oxidation of Ni; thus the negative going peak is much larger for $BaNiO_3$ then for NiOOH. The relatively good agreement between theory (one-shell calculations) and experiment here indicates that indeed the FEFF6 code correctly predicts the relative shifts in the edge with oxidation[18].

b. The agreement between theory and experiment for the $BaNiO_3$ - $Ni(OH)_2$ is comparable or even better for the 1 shell calculations than for the 2 and 9 shell calculations. Three possible reasons for this can be given. First, the 9-shell calculation contains over 100 atoms extending across 3 O-Ni-O slabs assuming perfect crystalline order. The worse agreement for the 9 shell calculations may arise from multi-slab contributions in the theory, which are suppressed in the experimental data because of non-registry of the slabs, irregularities in the gallery widths, or disorder in the galleries of the $Ni(OH)_2$ material. Second, it could arise

from an underestimate of the imaginary potential near the edge by the Hedin-Lundquest model utilized in these calculations, which would overestimate the contributions from the outer shells. We added a small imaginary potential (0.1 eV) to reduce this problem, but made little effort to optimize this value in this work. Finally, as the Ni-O bond gets stronger (i.e. decreases from $Ni(OH)_2$ to $BaNiO_3$), overlapping muffin-tin spheres may be required to provide better agreement with experiment as found previously by Hudson et al[25] for uranyl fluoride.

c. The agreement between the theory and experiment for the 1-shell calculations is remarkable considering that the average magnitude of the differences in the data amount to around 10-20% of the total absorption coefficient as shown in Fig. 1.

d. A feature growing in intensity around 25 eV with oxidation is known to arise from a many-body charge-transfer shakeup excitation, and therefore is not reproduced by the FEFF6 calculations[26]. We will discuss this shakeup feature and the significance of its growth elsewhere[20,27].

In light of the excellent agreement between the single-shell FEFF6 results and the experimental results obtained for the standard materials in Fig. 2, we proceed to compare results for the charged electrode with β-NiOOH; i.e., we examine μ(CE)-μ(β-NiOOH). This suggests comparison of various $[nlms]_t$ and $[3l,3s]_t$ single-shell calculations, since we have shown in Fig. 2 that the $[3l,3s]_t$ FEFF6 line shape approximates the NiOOH experimental line shape.. Figure 3 compares several single shell FEFF6 calculations to determine the effect of the number of short vs. long bonds (i.e., Ni oxidation level) and the uniformity of their distribution. These calculations clearly show a strong increase in the

amplitude of the oscillations with decreasing average bond length, d_{ave}, (i.e., increasing Ni oxidation) but the wavelength of the oscillations is surprisingly independent of d_{ave}. The difference spectra $([2l,4s]_t + [4l,2s]_t)/2 - [3l,3s]_t$, which compares configurations having the same d_{ave} and bond arrangement (i.e. trans in all cases) but with non-uniform distribution has very small amplitude (less than 2%). Unfortunately, this means that we can shed little light on the uniformity of the H atom distribution, however, the amplitude of the difference spectra gives a good measure of d_{ave}, or the average Ni oxidation.

Figure 3 also shows a comparison between the experimental spectra μ(CE) - μ(NiOOH) with the appropriate FEFF6 calculations on single-shell NiO_6 clusters. Based on examination of the $[nl,ms]_t$ results above, we conclude that the experimental line shape should be reasonably well approximated by the $[2l,4s]_t$ - $[3l,3s]_t$ FEFF6 line shape. This then provides evidence that the charged electrode is oxidized beyond that in NiOOH (Ni^{+3}); namely containing some $NiOOH_{0.67}$ (i.e., $Ni^{+3.3}$) consistent with the [2l,4s] configuration.

Although reasonable agreement in the line shapes exist between the $[2l,4s]_t$ - $[3l,3s]_t$ FEFF6 line shape and the experiential difference spectra, the amplitude of the oscillations in the $[2l,4s]_t$ - $[3l,3s]_t$ theory is smaller than in the experimental line shape. We emphasize again that the amplitudes in Fig. 3 are absolute (note that they are smaller here than in Fig. 2 because we are comparing here the charged electrode with β-NiOOH, which are more similar than β-$Ni(OH)_2$ and β-NiOOH compared in Fig. 2). Since the amplitudes are rather strongly dependent on $d_{ave.}$, this indicates that indeed some Ni with 6

short bonds (i.e., Ni^{+4}) exist in the charged electrode. This would be consistent with the NEXAFS edge data previously reported[9].

If the average oxidation state is indeed 3.5 in the charged electrode, and this contains a mix of $Ni^{+3.3}$ and Ni^{+4}, we would expect the line shape to be represented by $0.7[2l,4s]_t + 0.3[0l,6s]_t$. In Fig. 3, we compare this with the experimental difference line shape. The agreement is substantially improved by adding in the $[0l,6s] - [3l,3s]_t$ line shape confirming the presence of Ni^{+4} and that the average oxidation level is of the order of 3.5.

It is perhaps rather surprising that the amplitudes in the theory are too small since only small Debye-Waller factors ($\sigma^2 = 0.007$) were included here having a near negligible effect, and larger ones to reflect the possible disorder in the charged electrode would make the oscillations in the theory even smaller. If the Debye-Waller factors were increased, even larger amounts of Ni^{+4} would be indicated. This suggests that in the charged electrode the H atom distribution is well ordered, much more than in β-NiOOH. We will confirm this elsewhere[27].

Figure 4 examines the effect of the arrangement (cis or trans) of the long and short bonds about a Ni atom. Since we do not know the preferred arrangement in either the β-NiOOH or the charged electrode, we have 4 possible combinations (c-t, c-c, t-c, t-t). First we compare the FEFF6 results for the 4 combinations in the difference spectra. Note that the c-t and t-c combinations are the most different in the region between 15 and 28 eV, with the c-c and t-t combinations reflecting some average of these first two. This is the reason we utilized the t-t combination in Figs. 2 and 3. Fig. 4 now compares the optimal least squares fit of $x[0l,6s] + (1-x)[2l,4s]_{c/t} - [3l,3s]_{c/t}$ for the 4 combinations and compares

the sum of the squared deviations for these combinations. Although the c-t combination gives the best fit, it is not appreciatively better than the other combinations, so unfortunately these results are inconclusive. Nevertheless, all four optimal fits show that the [0l,6s] contribution is in the range of 25-40% with an average of around 33% consistent with a Ni oxidation slightly greater than 3.5 as indicated above.

The arrangement of the long and short bonds (i.e. cis or trans as discussed above) produces only an approximate 4-5% effect on the difference spectra as shown in Fig. 4. As a result only qualitative information on the H ordering in the gallery is possible at best. In previous calculations we have performed on $Zn(OH)_4$ and AlO_n (n = 4,5 or 6), even small distortions from tetrahedral and octahedral symmetry were clearly revealed[27]. Two reasons can be given for this. First, both the bond length arrangement and number of short bonds alter the line shape, and here for the Ni hydroxides the number of bonds has a larger affect, thus perhaps masking the dependence on the arrangement. Second, the geometric distortions in $Zn(OH)_4$ and AlO_n involved deviations of the angle subtended by the "ligand" atoms (i.e., 90° in the octahedral or 109° in the tetrahedral), while here we are dealing with the bond length arrangement. Hudson et al[25] have recently shown that multiple scattering "resonances" can arise within short O-M-O axial bonds. These resonant features apparently dissipate rapidly upon removal of the axial configuration (i.e., angle distortion). Thus, the NEXAFS spectra can be somewhat more sensitive to angle distortions then to bond length arrangement. FEFF6 calculations (not shown) confirm this. A 10% distortion in the bond angles ($[6l,0s]_{distorted}$ - [6l,0s]) produces amplitudes of

magnitude 15%, compared with 4-5 % resulting from the c/t bond arrangement ($[2l,4s]_t$-$[2l,4s]_c$).

Finally, we note that the differences between the optimum theoretical fit and the experimental line shapes around 20-30 eV for the charged electrode in Fig. 4 are very similar to those found for $BaNiO_3$ in Fig. 2. We believe these differences arises from the charge-transfer satellite present around 27 eV and the effect of this satellite on the line shape throughout the 20-30 eV region. Indeed, in Figs. 3 and 4, the small feature around 27 eV reflects the increased satellite in the charged electrode compared with β-NiOOH, giving further evidence that the charged electrode is in a higher oxidation state than β-NiOOH.

4. SUMMARY

A quantitative interpretation of Ni K-edge NEXAFS data for various Ni hydroxides utilizing the FEFF6 code reveals the following:

a. The FEFF6 code can reproduce the changes with oxidation remarkably well.

b. The intensity of the charge transfer shakeup peak increases with oxidation. This many-body satellite, not reproduced by the calculations, decreases the quality of the agreement with experiment in the 20-30 eV region.

c. FEFF6 calculations indicate that the amplitude of the oscillations in the difference spectra is directly proportional to the average Ni-O bond length, and hence directly reflects the average oxidation state of the Ni atom.

d. The difference spectra, relatively insensitive to the cis/trans arrangement of the short and long bonds about a Ni atom, provide only qualitative and tentative information on the ordering and arrangement of the H atoms in the galleries of these Ni materials.

e. The NEXAFS line shape indicates that some Ni^{+4} (i.e.,[0l,6s] coordination) exists along with $Ni^{+3.3}$ ([2l,4s] coordination) in the charged electrode, giving an average Ni oxidation state slightly greater than 3.5, consistent with that shown previously from the edge shift.

FIGURE CAPTIONS

1. Comparison of the Ni K-edge experimental NEXAFS data (μ) for β-$Ni(OH)_2$, β-NiOOH, and $BaNiO_3$, and an *in situ* charged electrode as previously published by O'Grady et al[9].

2. Comparison of experimental difference spectra [μ - $\mu(Ni(OH)_2$] with results obtained from curved-wave multiple scattering calculations (FEFF6 results) on cluster containing 1,2 and 9 shells approximating β-$Ni(OH)_2$ and $BaNiO_3$. The single shell calculations can be denoted by the notation [0l,6s] - [6l,0s] and $[3l,3s]_t$-[6l,0s] for the Ni^{+4} and Ni^{+3} cases respectively.

3. TOP - Comparison of $[nl,ns]_t$ - $[3l,3s]_t$ FEFF6 difference spectra showing the increase in amplitude with increasing d_{ave}.

   MIDDLE - Comparison of experimental difference spectra [μ(CE)-μ(β-NiOOH)] with $[2l,4s]_t$ - $[3l,3s]_t$ FEFF6 results.

   BOTTOM - Comparison of μ(CE) - μ(β-NiOOH) with 0.3[0l,6s] + 0.7$[2l,4s]_t$ - $[3l,3s]_t$ FEFF6 results.

4. TOP - Comparison of the $[2l,4s]_{c/t}$-$[3l,3s]_{c/t}$ FEFF6 results for the 4 possible cis/trans arrangements (c-c, c-t, t-c, and t-t) of the long and short Ni-O bonds about a single Ni atom.

BOTTOM - Comparison of the least squares fit of x [0l,6s] + (1-x)$[2l,4s]_{c/t}$ - $[3l,3s]_{c/t}$ to the experimental results, μ(CE)-μ(β-NiOOH) (solid line), for the four cis/trans combinations. The ledger shows the optimum value of x, and the sum of the squared deviations ($\Sigma\delta^2$) for each combination.

REFERENCES

1. P. Oliva, J. Leonardi, J.F. Laurent, E. Demas, J.J. Braconis, M. Figlanz, F. Fievet, and A. Deguibert, J. Power Sources **8**, 229 (1982).
2. F.T. Bacon, J. Electrochem. Soc **126**, 7C (1979).
3. D.E. Hall, J. Electrochem. Soc. **130** 317 (1983).
4. M.K. Carpenter, R.S. Conell, D.A. Corrigan, Solar Energy Mat. **16**, 333 (1987).
5. J.F. Jackovitz, in "The Nickel Electrode", R.G. Gunther and S. Gross, Eds. p. 48, The Electrochemical Society Softbound Processing Series, PV 82-84, Pennington, NJ (1982).
6. J. Desilvestro, D.A. Corrigan, and M.J. Weaver, J. Electrochem. Soc. **135**, 885 (1988).
7. C.A. Melendres, W. Paden, B. Tani, and W. Walczak, J. Electrochem. Soc. **134**, 762 (1987).
8. C. Greaves, M.A. Thomas, and M. Turner, in "Power Sources 9" J. Thompson, Ed. Acad. Press, New York, (1983).
9. W.E. O'Grady, K.I. Pandya, K.E. Swider, and D.A. Corrigan, J. Electrochem. Soc., to be published.
10. A.N. Mansour, C.A. Melendres, M. Pankuch, and R.A. Brizzolara, J. Electrochem. Soc. **141**, L69 (1994).
11. K.I. Pandya, W.E. O'Grady, D.A. Corrigan, J. McBreen, and R.W. Hoffman, J. Phys. Chem. **94**, 22 (1990);.

12. K.I. Pandya, R.W. Hoffman, J. McBreen, and W.E. O'Grady, J. Electrochem. Soc. **137**, 383 (1990)

13. J. McBreen, W.E. O'Grady, G. Tourillon, E. Dartyge, A. Fontaine, and K.I. Pandya, J. Phys. Chem. **93**, 6308 (1989).

14. D.A. Corrigan and S.L. Knight, J. Electrochem. Soc. **136**, 613 (1989).

15. J. McBreen in "Modern Aspects of Electrochemistry", R.E. White, J. O'M. Bockris, and B.E. Conway, eds., Plenum Press, New York (1990), Vol. 21, P. 29.

16. R.A. Huggins, H. Prinz, M. Wohlfahrt-Mehrens, L. Jorissen, and W. Witschel, Solid State Ionics **70/71**, 417 (1994).

17. Y. Takeda, F. Kanamaran, and M. Koizumi, Acta. Cryst. **B32**, 2464 (1976)

18. H.Sambe, X. Qian, T. Nabi, D.E. Ramaker, W.E. O'Grady, and A.N. Mansour, unpublished

19. X. Qian, H. Sambe, and D.E. Ramaker, Phys. Rev. B, in press.

20. D.E. Ramaker, H. Sambe, X. Qian, and W.E. O'Grady, Physica B **208/209** 49 (1995).

21. H. Sambe, X. Qian, and D.E. Ramaker, Phys. Rev. B (In press).

22. J.J. Rehr and R.C. Albers, Phys. Rev. **B41**, 8139 (1990).

23. J.J. Rehr, S.I. Zabinsky, A. Ankudinov, and R.C. Albers, Physica B, **208/209**, 23 (1995).

24. S.I. Zabinsky, J.J. Rehr, A. Ankudinov, R.C. Albers, and M.J. Eller, in press.

25. E.A. Hudson, J.J. Rehr, and J.J. Bucher, Physical Review, in press.

26. E.A. Stern, Phys. Rev. Lett., **Vol. 49**, No 18, 1353 (1982); J.J. Rehr, E.A. Stern, R.L. Martin, and E.R. Davidson, Phys. Rev. **B17**, 560 (1978).

27. X. Qian, H. Sambe, D.E. Ramaker, and W.E. O'Grady, unpublished.

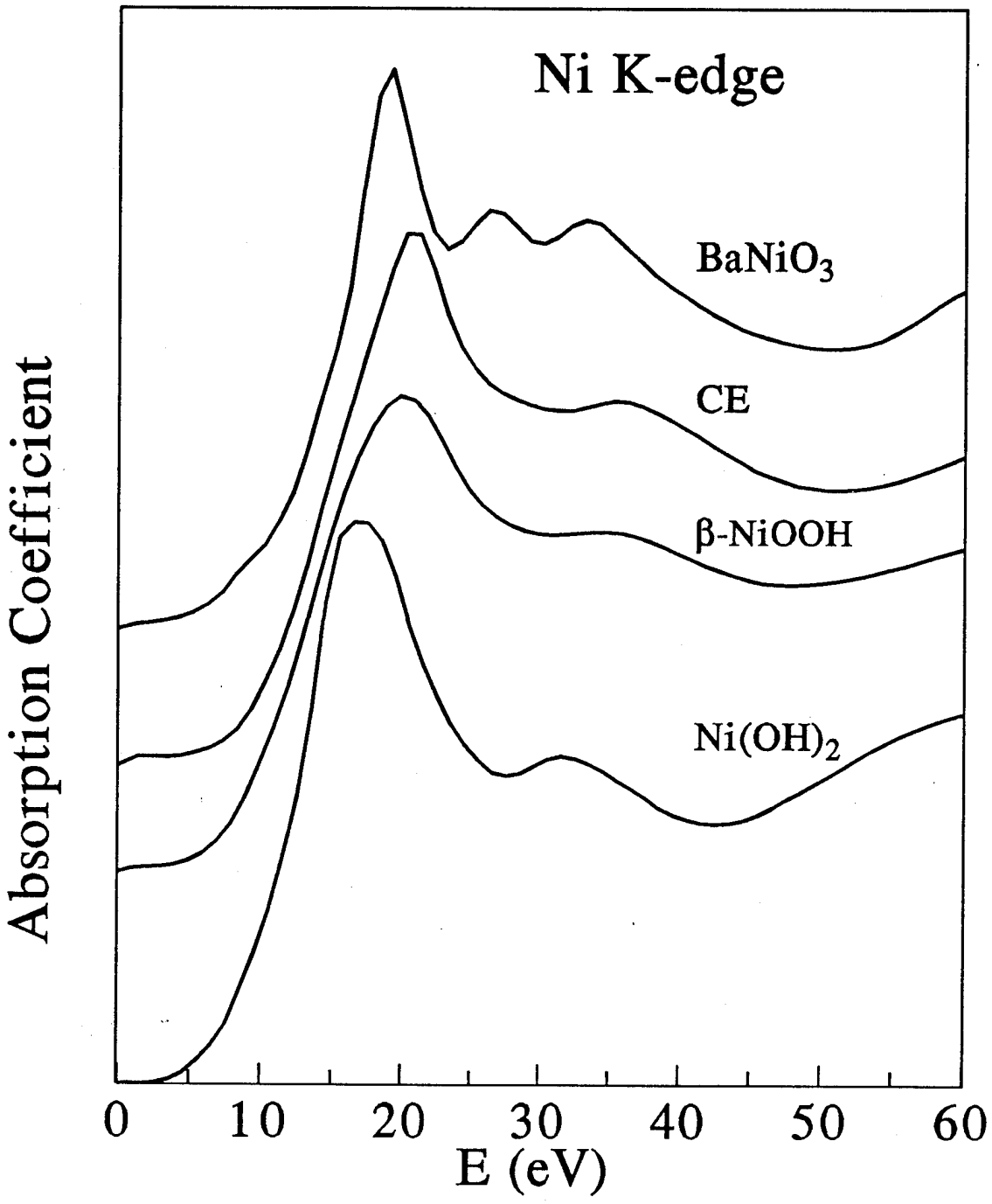
Ni K-edge
BaNiO3
CE
β-NiOOH
Ni(OH)2
Absorption Coefficient
0
10
20
30
40
50
60
E (eV)

Fig 1

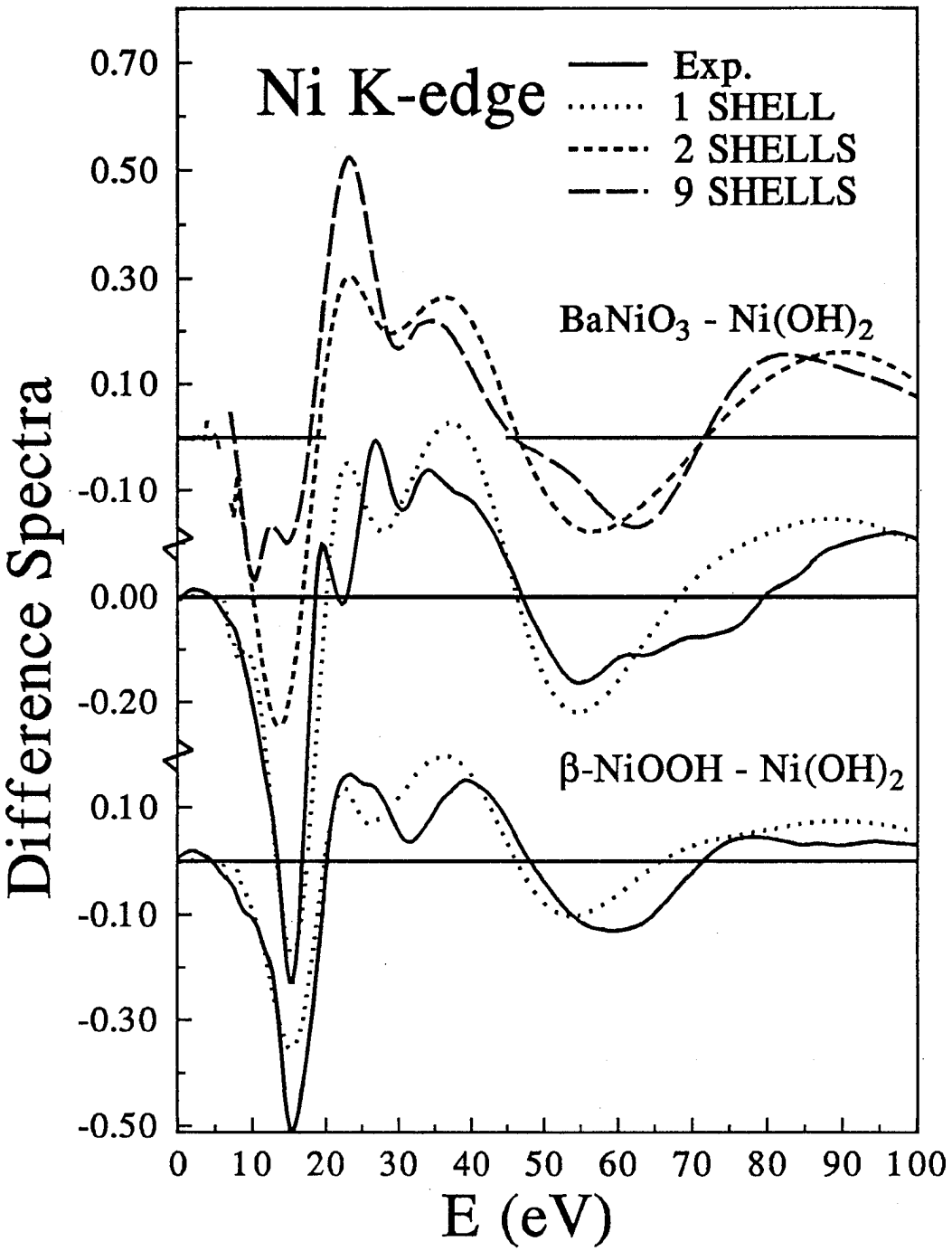
Ni K-edge
Exp.
1 SHELL
2 SHELLS
9 SHELLS
BaNiO3 - Ni(OH)2
β-NiOOH - Ni(OH)2
Difference Spectra
E (eV)
0.70
0.50
0.30
0.10
-0.10
0.00
-0.20
0.10
-0.10
-0.30
-0.50
0
10
20
30
40
50
60
70
80
90
100

Fig 2

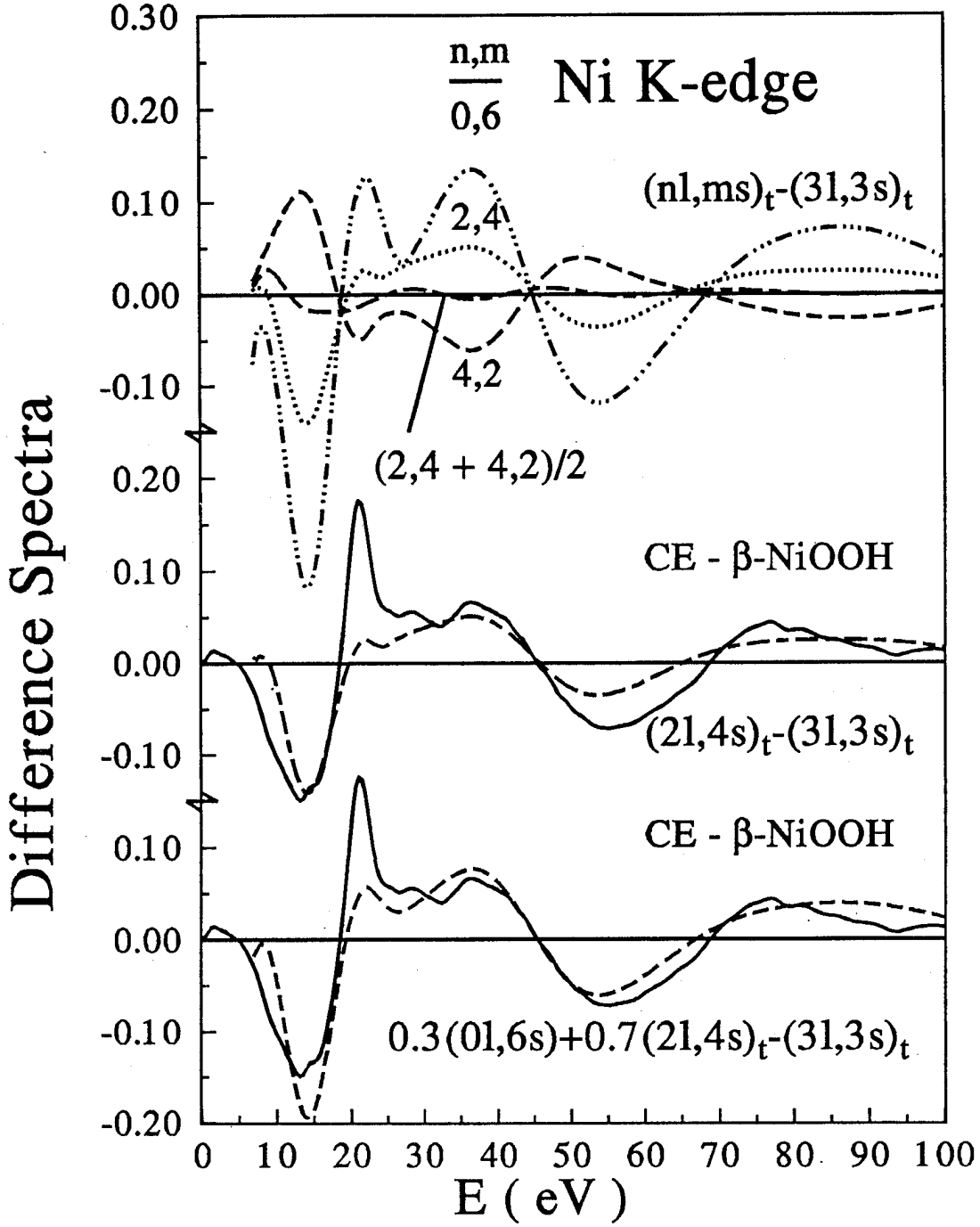
Ni K-edge
n,m
0,6
(nl,ms)t-(31,3s)t
2,4
4,2
(2,4 + 4,2)/2
CE - β-NiOOH
(21,4s)t-(31,3s)t
CE - β-NiOOH
0.3(01,6s)+0.7(21,4s)t-(31,3s)t
Difference Spectra
E (eV)
0.30
0.20
0.10
0.00
-0.10
0.20
0.10
0.00
-0.10
0.10
0.00
-0.10
-0.20
0 10 20 30 40 50 60 70 80 90 100

Fig. 3

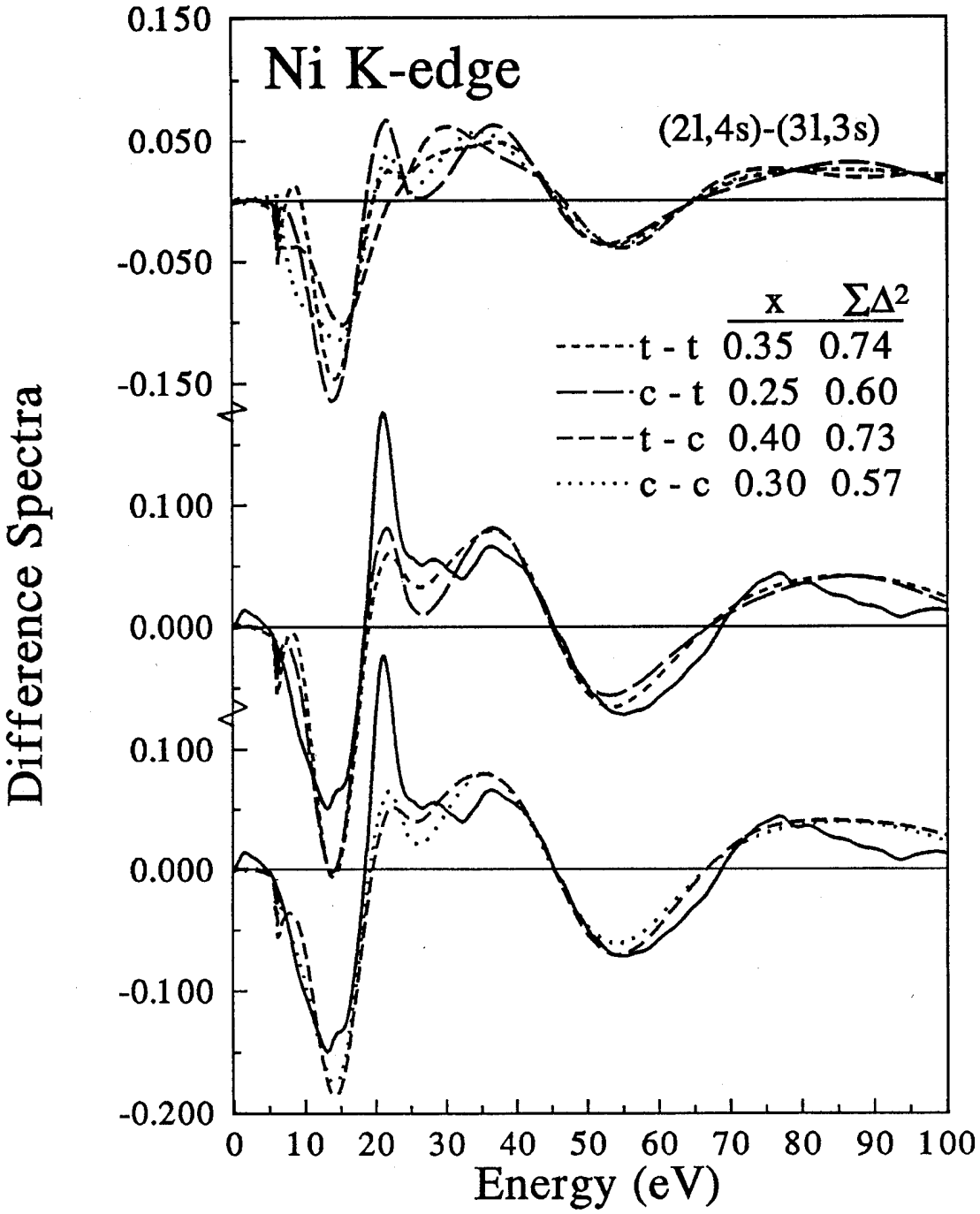
Ni K-edge
(21,4s)-(31,3s)
x ΣΔ²
t - t 0.35 0.74
c - t 0.25 0.60
t - c 0.40 0.73
c - c 0.30 0.57
Difference Spectra
Energy (eV)
0.150
0.050
-0.050
-0.150
0.100
0.000
0.100
0.000
-0.100
-0.200
0 10 20 30 40 50 60 70 80 90 100

Fig. 4

Technical Report Distribution List

Dr. Robert J. Nowak (1)*
ONR 331
800 N. Quincy St.
Arlington, VA 22217-5660

Defense Technical Information Ctr (2) **
Building 5, Cameron Station
Alexandria, VA 22314

Dr. James S. Murday (1)
Chemistry Division, NRL 6100
Naval Research Laboratory
Washington, DC 20375-5660

Dr. John Fischer (1)
Chemistry Division, Code 385
NAWCWD - China Lake
China Lake, CA 93555-6001

Dr. Peter Seligman (1)
NCCOSC - NRAD
San Diego, CA 92152-5000

Dr. James A. Gucinski (1)
NSWC Code 609
300 Highway 361
Crane, IN 47522-5001

Mr. Christopher Egan (1)
Naval Undersea Warfare Center
Division Newport
1176 Howell St.
Newport, RI 02841-1708

Dr. Carl Mueller
Naval Surface Warfare Center - White Oak
Code R36
10901 New Hampshire Ave.
Silver Spring, MD 20903-5640

* Number of copies required